Author disclosures are available with the text of this letter at www.atsjournals.org.

Acknowledgment: The authors thank C. Hendry for rigorous and thorough manuscript edits, J. Avolio for help with nasal cell scrapings, A. Fitzpatrick for help with high-speed video microscopy acquisition, and M. A. Seibold for healthy control samples.

Maurizio Chioccioli, Ph.D.
University of Cambridge
Cambridge, United Kingdom
and
Yale University School of Medicine
New Haven, Connecticut

Luigi Feriani, Ph.D.
University of Cambridge
Cambridge, United Kingdom
and
Imperial College London
London, United Kingdom

Quynh Nguyen, M.Sc.
University of Toronto
Toronto, Ontario, Canada

Jurij Kotar, Ph.D.
University of Cambridge
Cambridge, United Kingdom

Sharon D. Dell, M.D., B.Eng.
University of Toronto
Toronto, Ontario, Canada

Vito Mennella, Ph.D.
University of Toronto
Toronto, Ontario, Canada
and
SickKids Hospital
Toronto, Ontario, Canada

Israel Amirav, M.D.
University of Alberta
Edmonton, Alberta, Canada

Pietro Cicuta, Ph.D.*
University of Cambridge
Cambridge, United Kingdom

ORCID ID: 0000-0002-9193-8496 (P.C.).

*Corresponding author (e-mail: pc245@cam.ac.uk).

References

1. Lucas JS, Barbato A, Collins SA, Goutaki M, Behan L, Caudri D, *et al*. European Respiratory Society guidelines for the diagnosis of primary ciliary dyskinesia. *Eur Respir J* 2017;49:1601090.
2. Pifferi M, Michelucci A, Conidi ME, Cangiotti AM, Simi P, Macchia P, *et al*. New DNAH11 mutations in primary ciliary dyskinesia with normal axonemal ultrastructure. *Eur Respir J* 2010;35:1413–1416.
3. Schwabe GC, Hoffmann K, Loges NT, Birker D, Rossier C, de Santi MM, *et al*. Primary ciliary dyskinesia associated with normal axoneme ultrastructure is caused by DNAH11 mutations. *Hum Mutat* 2008;29:289–298.
4. Olbrich H, Schmidts M, Werner C, Onoufriadis A, Loges NT, Raidt J, *et al*.; UK10K Consortium. Recessive HYDIN mutations cause primary ciliary dyskinesia without randomization of left-right body asymmetry. *Am J Hum Genet* 2012;91:672–684.
5. Davis SD, Ferkol TW, Rosenfeld M, Lee HS, Dell SD, Sagel SD, *et al*. Clinical features of childhood primary ciliary dyskinesia by genotype and ultrastructural phenotype. *Am J Respir Crit Care Med* 2015;191: 316–324.
6. Bruot N, Cicuta P. Realizing the physics of motile cilia synchronization with driven colloids. *Annu Rev Condens Matter Phys* 2016;7:323–348.
7. Brumley DR, Wan KY, Polin M, Goldstein RE. Flagellar synchronization through direct hydrodynamic interactions. *Elife* 2014;3:e02750.
8. Raidt J, Wallmeier J, Hjeij R, Onnebrink JG, Pennekamp P, Loges NT, *et al*. Ciliary beat pattern and frequency in genetic variants of primary ciliary dyskinesia. *Eur Respir J* 2014;44:1579–1588.
9. Olbrich H, Häffner K, Kispert A, Völkel A, Volz A, Sasmaz G, *et al*. Mutations in DNAH5 cause primary ciliary dyskinesia and randomization of left-right asymmetry. *Nat Genet* 2002;30: 143–144.

Copyright © 2019 by the American Thoracic Society

Perfusion Imaging Distinguishes Exercise Pulmonary Arterial Hypertension at Rest

To the Editor:

Recent attempts have been made to define abnormal pulmonary pressure during exercise (1). However, it is unclear whether exercise pulmonary arterial hypertension (ePAH)—defined here by *1*) normal mean pulmonary artery pressure (mPAP) at rest, *2*) elevation of mPAP (>30 mm Hg) with exercise, and *3*) normal left ventricular filling pressures during exercise—represents a pathologic change of the pulmonary vasculature. Indeed, no resting measurement to date has revealed any anatomic or physiological abnormality in patients with ePAH.

Here, we applied positron emission tomography (PET) imaging using the ^{13}NN-saline bolus method (2) to investigate vascular changes in subjects with ePAH. We hypothesized that pulmonary perfusion imaging conducted at rest before and after eliminating pulmonary vascular tone with inhaled nitric oxide (iNO) and hyperoxia would distinguish characteristic perfusion patterns among patients with ePAH and PAH, and control subjects. Some of the results of this study have been previously reported in the form of an abstract (3).

Methods

We studied five control subjects, four subjects with ePAH, and four subjects with PAH who underwent intravenous-bolus ^{13}NN-saline functional PET imaging of pulmonary perfusion in the supine

Supported by an unrestricted grant from United Therapeutics. The sponsor was not involved in the study design, analysis, or reporting of study findings.

Author Contributions: Study design: E.G.K., M.K., R.C., and R.S.H. Data acquisition: P.K., V.J.K., E.G.K., J.R.-L., K.A.H., M.K., D.M.S., J.G.V., R.C., T.W., and R.S.H. Data analysis: P.K., V.J.K., T.W., and R.S.H. Data interpretation: P.K., T.W., and R.S.H. Manuscript drafting and editing: P.K., V.J.K., T.W., and R.S.H. Final manuscript approval: P.K., V.J.K., E.G.K., J.R.-L., K.A.H., M.K., D.M.S., A.B.W., J.G.V., R.C., T.W., and R.S.H. Agreement to be accountable for the work: P.K., V.J.K., E.G.K., J.R.-L., K.A.H., M.K., D.M.S., A.B.W., J.G.V., R.C., T.W., and R.S.H.

Originally Published in Press as DOI: 10.1164/rccm.201810-1899LE on February 27, 2019

position, using previously described methods (2, 4, 5). Briefly, the total spatial heterogeneity of perfusion [CV^2_{Qtotal} = (SD of perfusion/average perfusion)^2] was assessed at baseline and while the subjects were breathing 30 ppm iNO and oxygen (O_2 + iNO) to eliminate resting vascular tone, thereby leaving structural abnormalities as the primary driver of perfusion differences among the subjects. The additive components of CV^2_{Qtotal} included the contributions of *1*) the vertical (dorsoventral) gradient in perfusion (CV^2_{Qvgrad}), *2*) the axial (craniocaudal) gradient in perfusion (CV^2_{Qzgrad}), and *3*) the residual heterogeneity (CV^2_{Qr}). The residual heterogeneity in perfusion (CV^2_{Qr}) was calculated by subtracting the heterogeneity caused by both the vertical gradient and the axial gradient in perfusion from the total heterogeneity (CV^2_{Qr} = $CV^2_{Qtotal} - CV^2_{Qvgrad} - CV^2_{zgrad}$). The remaining CV^2_{Qr} was subsequently binned into contributions calculated at different image resolutions (length scales) (2, 6). Overall, small length scales starting at 10 mm correspond to variation among volumes of approximately 1 ml (5 acinar units), whereas large length scales correspond to variation among larger regions such as segments and subsegments.

We first conducted a one-way ANOVA and then tested simultaneous comparisons with multiple-hypothesis testing correction using the Tukey-Kramer method (SAS for Windows, version 9.4; SAS Institute Inc.). Statistical significance was set at $P < 0.05$.

Results

The baseline characteristics of the study population are displayed in Table 1. All of the subjects were nonsmokers without prior cardiovascular disease and without evidence of lung disease by high-resolution computed tomography. No subjects required oxygen therapy. Subjects with ePAH had normal resting mPAP (mean, 18 [range, 15–22] mm Hg) and pulmonary capillary wedge pressure (PCWP 9 [7–11] mm Hg), and an elevated mPAP with exercise (36 [33–38] mm Hg). Subjects with ePAH had a mean pulmonary vascular resistance [(mPAP − PCWP)/cardiac output] during exercise of 154.6 (136–168) dyn · s/cm^5. According to recent European Respiratory Society standards for assessing pulmonary hemodynamics during exercise, all subjects with ePAH had a total pulmonary resistance (mPAP/cardiac output) of >3.0 (1) Wood units during exercise while maintaining a PCWP of <20 mm Hg, except for one subject who had a total pulmonary resistance of 2.3 Wood units.

^{13}NN-saline functional PET imaging revealed perfusion characteristics that distinguished all groups. For instance, subjects with PAH had significantly attenuated vertical perfusion gradients (Q_{vgrad}) compared with subjects with ePAH and their control counterparts while breathing O_2 + iNO (Q_{vgrad} 10^{-2} cm^{-1}, PAH 2.51 ± 2.06 vs. ePAH 6.96 ± 0.62 vs. control 7.37 ± 0.86, $P_{ANOVA} < 0.001$). Subjects with ePAH, on the other hand, had perfusion gradients similar to those observed in control subjects but had significantly greater CV^2_{Qtotal} than both subjects with PAH and control subjects at baseline (CV^2_{Qtotal} baseline, ePAH 0.15 ± 0.04 vs. PAH 0.08 ± 0.02 vs. control 0.09 ± 0.04, $P_{ANOVA} < 0.02$), with further discrimination while breathing O_2 + iNO (CV^2_{Qtotal} breathing O_2 + iNO, ePAH 0.21 ± 0.04 vs. PAH 0.06 ± 0.03 vs. control 0.13 ± 0.03, $P_{ANOVA} < 0.0002$). After we subtracted the perfusion gradients, we found that the greater CV^2_{Qr} in subjects with ePAH was driving this increased CV^2_{Qtotal}. Furthermore, subjects with ePAH demonstrated greater perfusion heterogeneity across the components of CV^2_{Qr}, or different image resolutions (length scale spectrum 10–110 mm) ($P_{ANOVA} < 0.01$ for all length scales) compared with their control and PAH counterparts (Figure 1). After further adjustment for regional lung density by high-resolution computed tomography, these differences in perfusion within and between groups persisted.

Discussion

PET imaging revealed two unique perfusion characteristics in subjects with ePAH at rest. First, these subjects demonstrated a

Table 1. Baseline Characteristics

Parameter	Control (*n* = 5)	ePAH (*n* = 4)	PAH (*n* = 4)	*P* Value
Age, yr	41.2 (22–60)	53.5 (44–62)	47.3 (22–64)	0.52
Sex, F	1	2	3	0.31
Race, white	5	3	3	0.55
Height, cm	170.9 (160–181.6)	169.2 (167.6–180.3)	170.7 (167.6–174)	0.96
Weight, kg	86 (72.6–134.6)	88 (68–107)	77.3 (56.2–119.7)	0.85
Years of symptoms	–	4.2 (1–10)	8.4 (7–10)	0.19
FEV_1% predicted	103.7 (90–117)	87.9 (76–97)	82.9 (66–95)	0.12
FVC, % predicted	105.8 (100–115)	91.2 (83–118)	85.6 (64–110)	0.24
FEV_1/FVC	79 (70–87)	72 (67–89)	80 (63–86)	0.50
mPAP, rest, mm Hg	–	18 (15–22)	41.6 (33–63)	0.01
PVR, rest, dyn · s/cm^5	–	122.7 (81–143)	442 (322–548)	0.001
PCWP, rest, mm Hg	–	9.3 (7–11)	10 (7–16)	0.65
mPAP, exercise, mm Hg	–	36 (33–38)	–	–
PVR, exercise, dyn · s/cm^5	–	154.6 (136–168)	–	–
PCWP, exercise, mm Hg	–	14.3 (11–18)	–	–
6MWD, m	–	485.2 (366–595)	463.2 (382–670)	0.083

Definition of abbreviations: 6MWD = 6-minute-walk distance; ePAH = exercise pulmonary arterial hypertension; mPAP = mean pulmonary arterial pressure; PAH = primary pulmonary arterial hypertension; PCWP = pulmonary capillary wedge pressure; PVR = pulmonary vascular resistance.
Continuous variables are represented as mean (minimum–maximum). Categorical variables are represented as counts.

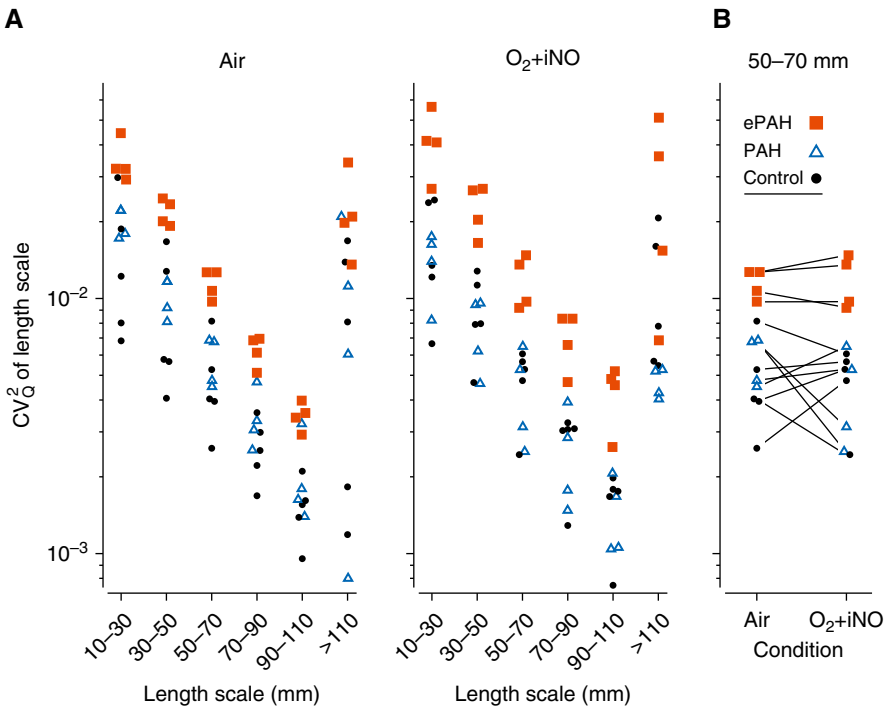

Figure 1. Subjects with ePAH had increased perfusion heterogeneity across image resolutions (length scales). The residual heterogeneity of perfusion (CV^2_{Qr}) is a component of the total spatial heterogeneity (CV^2_{Qtotal}), which also includes the vertical (dorsoventral) gradient in perfusion (CV^2_{Qvgrad}) and the axial (craniocaudal) gradient in perfusion (CV^2_{Qzgrad}), so that $CV^2_{Qr} = CV^2_{Qtotal} - CV^2_{Qvgrad} - CV^2_{zgrad.}$ The residual heterogeneity in perfusion (CV^2_{Qr}) was then split into components of heterogeneity captured at different image resolutions (length scales) (2, 6). The contribution of specific image resolution ranges to CV^2_{Qr} was calculated as the difference between two successive filter sizes, which is demonstrated in this figure for all subjects with ePAH and PAH, and control subjects. (*A*) The variation in perfusion at different image resolutions (length scales) revealed that subjects with ePAH had significantly greater perfusion heterogeneity at all image resolutions at baseline. This perfusion profile further discriminated subjects with ePAH from those with PAH and control subjects during O_2 + iNO. (*B*) Paired perfusion heterogeneity at the medium-sized image resolutions (length scale, $CV^2_{Q50–70}$) demonstrated that subjects with ePAH had greater perfusion heterogeneity than those with PAH and control subjects both before and during O_2 + iNO. $CV^2_{Q50–70}$ = squared coefficient of variation in perfusion quantifying the heterogeneity at the length scale of 50–70 mm; ePAH = exercise pulmonary arterial hypertension; O_2 +iNO = inhaled nitric oxide with balance gas oxygen; PAH = pulmonary arterial hypertension.

perfusion pattern characterized by increased spatial heterogeneity in perfusion across image resolutions (length scale spectrum 10–110 mm) at rest that distinguished them from both subjects with PAH and control subjects. Second, subjects with ePAH maintained a normal resting vertical gradient in perfusion that was responsive to vasodilation, similar to what was observed in their control counterparts but distinct from subjects with PAH.

We show for the first time that subjects with ePAH at rest have distinct perfusion characteristics at baseline and during pulmonary vasodilation (O_2 + iNO). Subjects with ePAH demonstrated greater total perfusion heterogeneity (CV^2_{Qtotal}) than control subjects and subjects with PAH. An examination of the components of CV^2_{Qtotal} revealed that subjects with ePAH had resting vertical and axial gradients and perfusion redistribution in response to O_2 + iNO similar to what was observed in control subjects, indicating low resting pulmonary vascular pressures and a normal vascular response to gravitational forces. However, subjects with ePAH demonstrated greater residual perfusion heterogeneity (CV^2_{Qr}) and greater heterogeneity regardless of image resolution or length scale spectrum (10–110 mm) than control subjects and subjects with PAH. Our observations suggest that subjects with ePAH have a higher spatial heterogeneity in perfusion across different sizes of anatomical and functional units among the branching regions of the vascular tree at rest, ranging from acinar-sized units represented at smaller image resolutions to segmental-sized units represented at larger image resolutions.

Although our findings are compelling, a key limitation should be considered. This was a small pilot study, but our observations of attenuated vertical perfusion gradients in subjects with PAH are consistent with prior observations (7). Additionally, accentuation of perfusion differences with O_2 + iNO further corroborates baseline perfusion differences, because if our result were due to chance alone, we would not have expected a systematic strengthening of the finding.

To date, no resting structural or functional measurement has been able to predict the symptomatic increases in mPAP at exercise that have been demonstrated in patients with ePAH (8). Although individuals with ePAH and PAH both have objective manifestations of exercise intolerance, including signs of increased right ventricular afterload and right ventricular/pulmonary vascular uncoupling (8, 9), the distinct mechanisms that are responsible for an increase in pulmonary

artery pressure during exercise in ePAH have been unclear. Dynamic pulmonary vasoconstriction has been previously implicated (9, 10); however, in comparison with control subjects and subjects with PAH, our findings show the presence of a distinct vascular pathology at rest in subjects with ePAH, represented by increased perfusion heterogeneity across image resolutions (length scale spectrum 10–110 mm). Whether this pattern heralds permanent vascular remodeling cannot be determined by our data, and a longitudinal study will be required to definitively evaluate whether this pathology relates to an intermediate PAH phenotype (10) or whether this unique perfusion pattern represents a distinct disease process. ■

Author disclosures are available with the text of this letter at www.atsjournals.org.

Puja Kohli, M.D., M.M.Sc.*
Massachusetts General Hospital and Harvard Medical School
Boston, Massachusetts

Vanessa J. Kelly, Ph.D.
Massachusetts General Hospital
Boston, Massachusetts

Ekaterina G. Kehl, M.D.
Josanna Rodriguez-Lopez, M.D.
Kathryn A. Hibbert, M.D.
Mamary Kone, M.P.H.
Massachusetts General Hospital and Harvard Medical School
Boston, Massachusetts

David M. Systrom, M.D.
Aaron B. Waxman, M.D.
Brigham and Women's Hospital and Harvard Medical School
Boston, Massachusetts

Jose G. Venegas, Ph.D.
Richard Channick, M.D.
Tilo Winkler, Ph.D.‡
R. Scott Harris, M.D.‡
Massachusetts General Hospital and Harvard Medical School
Boston, Massachusetts

ORCID ID: 0000-0002-7276-5550 (T.W.).

*Corresponding author (e-mail: pkohli1@mgh.harvard.edu).
‡These authors contributed equally to this work.

References

1. Kovacs G, Herve P, Barbera JA, Chaouat A, Chemla D, Condliffe R, *et al*. An official European Respiratory Society statement: pulmonary haemodynamics during exercise. *Eur Respir J* 2017;50: 1700578.
2. Vidal Melo MF, Winkler T, Harris RS, Musch G, Greene RE, Venegas JG. Spatial heterogeneity of lung perfusion assessed with (13)N PET as a vascular biomarker in chronic obstructive pulmonary disease. *J Nucl Med* 2010;51:57–65.
3. Kohli P, Winkler T, Kelly VJ, Gladysheva E, Kone M, Hibbert K, *et al*. EIPAH and PAH subjects have different regional perfusion patterns after vasodilation. *Am J Respir Crit Care Med* 2018;197: A4375.
4. Venegas JG, Winkler T, Musch G, Vidal Melo MF, Layfield D, Tgavalekos N, *et al*. Self-organized patchiness in asthma as a prelude to catastrophic shifts. *Nature* 2005;434:777–782.
5. Kelly VJ, Hibbert KA, Kohli P, Kone M, Greenblatt EE, Venegas JG, *et al*. Hypoxic pulmonary vasoconstriction does not explain all regional perfusion redistribution in asthma. *Am J Respir Crit Care Med* 2017; 196:834–844.
6. Motta-Ribeiro GC, Hashimoto S, Winkler T, Baron RM, Grogg K, Paula LFSC, *et al*. Deterioration of regional lung strain and inflammation during early lung injury. *Am J Respir Crit Care Med* 2018; 198:891–902.
7. Jones AT, Hansell DM, Evans TW. Quantifying pulmonary perfusion in primary pulmonary hypertension using electron-beam computed tomography. *Eur Respir J* 2004;23:202–207.
8. Naeije R, Vanderpool R, Dhakal BP, Saggar R, Saggar R, Vachiery J-L, *et al*. Exercise-induced pulmonary hypertension: physiological basis and methodological concerns. *Am J Respir Crit Care Med* 2013;187:576–583.
9. Vanderpool RR, Pinsky MR, Naeije R, Deible C, Kosaraju V, Bunner C, *et al*. RV-pulmonary arterial coupling predicts outcome in patients referred for pulmonary hypertension. *Heart* 2015;101:37–43.
10. Oudiz RJ, Rubin LJ. Exercise-induced pulmonary arterial hypertension: a new addition to the spectrum of pulmonary vascular diseases. *Circulation* 2008;118:2120–2121.

Copyright © 2019 by the American Thoracic Society

Is Nitric Oxide Nephro- or Cardioprotective?

To the Editor:

We read with interest the article recently published in the *Journal* by Lei and colleagues entitled "Nitric Oxide Decreases Acute Kidney Injury and Stage 3 Chronic Kidney Disease after Cardiac Surgery" (1). In a single-center, prospective, randomized, controlled trial, the authors compared inhaled nitric oxide (NO) versus inhaled nitrogen (N_2), administered via the gas exchanger during cardiopulmonary bypass and then by inhalation for 24 hours postoperatively, in adult patients undergoing multiple-valve cardiac surgery. A total of 244 patients were included. Inhaled NO was associated with a lower incidence of acute kidney injury (50% in the NO group vs. 64% in the control group; relative risk, 0.78; 95% confidence interval, 0.62–0.97; $P = 0.014$). These findings might appear to contrast with previously published literature suggesting that NO is nephrotoxic (2).

Inhaled NO-associated renal injury has been suggested to result from tissue hypoxia and oxidative stress through NO by-products, including methemoglobin, NO_2^-, and NO_3^- (3). In the present study, the authors suggest that the nephroprotective effect of inhaled NO would arise from the prevention of plasma depletion of NO secondary to circulating plasma hemoglobin, thereby preserving microvascular perfusion. Plasma hemoglobin oxidation by NO inhalation could also reduce free hemoglobin–related toxicity to the kidney. This is, however, highly speculative. We propose a unifying mechanism that may account for some degree of nephroprotection in this setting, i.e., a cardioprotective effect. Right ventricular dysfunction is common after cardiopulmonary bypass and has been found to be associated with renal dysfunction (4). Many experimental and

This article is open access and distributed under the terms of the Creative Commons Attribution Non-Commercial No Derivatives License 4.0 (http://creativecommons.org/licenses/by-nc-nd/4.0/). For commercial usage and reprints, please contact Diane Gern (dgern@thoracic.org).

Originally Published in Press as DOI: 10.1164/rccm.201812-2344LE on March 6, 2019